HHS Public Access

Author manuscript

Cell Rep. Author manuscript; available in PMC 2022 June 21.

Published in final edited form as:

Cell Rep. 2022 May 17; 39(7): 110817. doi:10.1016/j.celrep.2022.110817.

Toll-9 interacts with Toll-1 to mediate a feedback loop during apoptosis-induced proliferation in *Drosophila*

Alicia Shields[1,4],

Alla Amcheslavsky[1,4],

Elizabeth Brown[1],

Tom V. Lee[2],

Yingchao Nie[3],

Takahiro Tanji[3],

Y. Tony Ip[3],

Andreas Bergmann[1,5,*]

[1]Department of Molecular, Cell and Cancer Biology, University of Massachusetts Medical School, Worcester, MA 01605, USA

[2]Department of Neurology, Baylor College of Medicine, Houston, TX 77030, USA

[3]Program in Molecular Medicine, University of Massachusetts Medical School, Worcester, MA 01605, USA

[4]These authors contributed equally

[5]Lead contact

SUMMARY

Drosophila Toll-1 and all mammalian Toll-like receptors regulate innate immunity. However, the functions of the remaining eight Toll-related proteins in *Drosophila* are not fully understood. Here, we show that *Drosophila* Toll-9 is necessary and sufficient for a special form of compensatory proliferation after apoptotic cell loss (undead apoptosis-induced proliferation [AiP]). Mechanistically, for AiP, Toll-9 interacts with Toll-1 to activate the intracellular Toll-1 pathway for nuclear translocation of the NF-κB-like transcription factor Dorsal, which induces expression of the pro-apoptotic genes *reaper* and *hid*. This activity contributes to the feedback amplification loop that operates in undead cells. Given that Toll-9 also functions in loser cells

*Correspondence: andreas.bergmann@umassmed.edu.

AUTHOR CONTRIBUTIONS

Conceptualization, A.A., A.S., and A.B.; Methodology, A.A., A.S, and E.B.; Validation, A.A. and A.S.; Investigation, A.A., A.S., and E.B.; Resources, T.V.L., Y.N., T.T., and Y.T.I.; Writing – Original Draft, A.B.; Writing – Review & Editing, A.B.; Visualization, A.B.; Supervision, A.B. and Y.T.I.; Funding Acquisition, A.B. and Y.T.I.

DECLARATION OF INTERESTS

The authors declare no competing interest.

INCLUSION AND DIVERSITY

One or more of the authors of this paper self-identifies as an underrepresented ethnic minority in science.

SUPPLEMENTAL INFORMATION

Supplemental information can be found online at https://doi.org/10.1016/j.celrep.2022.110817.

during cell competition, we define a general role of Toll-9 in cellular stress situations leading to the expression of pro-apoptotic genes that trigger apoptosis and apoptosis-induced processes such as AiP. This work identifies conceptual similarities between cell competition and AiP.

In brief

Shields et al. define a general role of Toll-9 in cellular stress situations leading to the expression of pro-apoptotic genes that trigger apoptosis and apoptosis-induced processes such as apoptosis-induced proliferation. This work identifies conceptual similarities between cell competition and apoptosis-induced proliferation.

Graphical Abstract

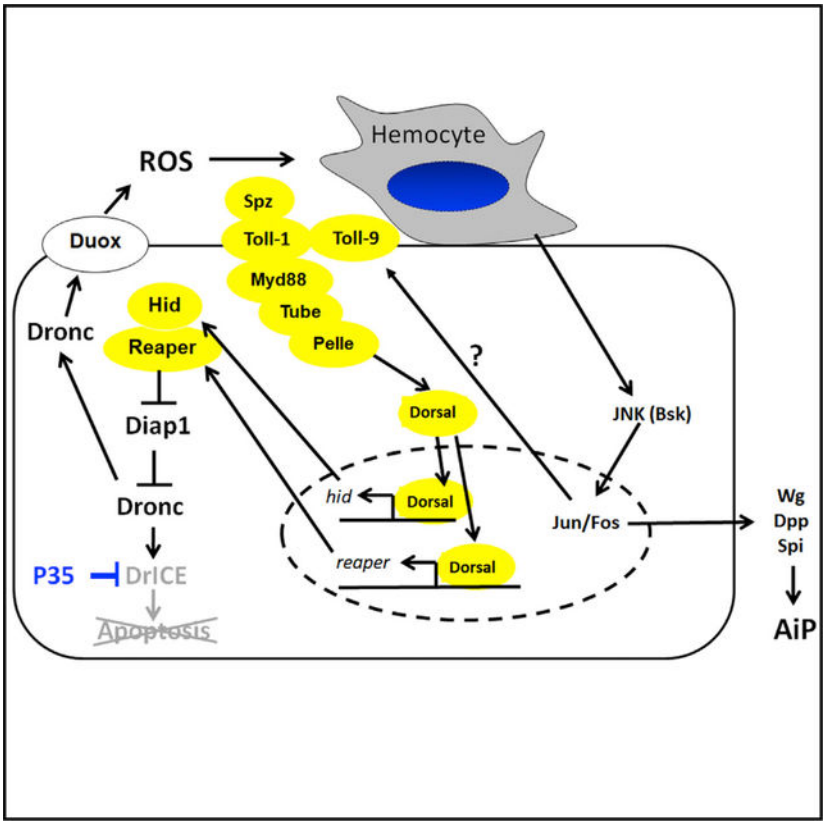

INTRODUCTION

Since the discovery of the original *Toll* gene in *Drosophila* (*Toll-1* hereafter), a large number of *Toll*-related genes have been identified in both insects and mammals (reviewed in Anthoney et al., 2018; Bilak et al., 2003). The *Drosophila* genome encodes a total of 9 *Toll*-related genes, including *Toll-1* (Ooi et al., 2002; Tauszig et al., 2000), while mammalian genomes encode between 10 and 13 Toll-like receptors (TLRs). TLRs are single-pass transmembrane proteins that upon ligand stimulation usually trigger a conserved intracellular signaling pathway, culminating in the activation of NF-κB transcription factors (Anthoney et al., 2018).

Initially identified as an essential gene for dorsoventral patterning in the early *Drosophila* embryo (Anderson et al., 1985a, 1985b) (reviewed by Nusslein-Volhard, 2021), *Toll-1* was later also found to be a critical component for innate immunity (Lemaitre, 2004; Lemaitre et al., 1996). In this function, Toll-1 signaling via the NF-κB transcription factors Dorsal and Dorsal-related immunity factor (Dif) induces the expression of anti-microbial peptides (AMPs) that mediate innate immunity (Meng et al., 1999; Rutschmann et al., 2000; Tauszig et al., 2000). A role in innate immunity has also been demonstrated for all mammalian TLRs (Lemaitre, 2004). Likewise, *Drosophila* Toll-8 (aka Tollo) regulates immunity in the trachea (Akhouayri et al., 2011). Toll-7 may regulate anti-viral responses, albeit through an NF-κB-independent mechanism (Benton et al., 2016; Lamiable et al., 2016; Nakamoto et al., 2012; Pare et al., 2014). However, for the remaining Toll-related proteins in *Drosophila*, a function in innate immunity has not been clearly demonstrated (Anthoney et al., 2018; Tauszig et al., 2000).

Of particular interest is Toll-9 in *Drosophila* because it behaves genetically most similar to *Toll-1* (Bettencourt et al., 2004; Ooi et al., 2002), and its intracellular TIR domain is most closely related to those of the mammalian TLRs (Khush and Lemaitre, 2000; Ooi et al., 2002; Wasserman, 2000). Overexpression of *Toll-9* results in the production of AMPs, which led to the proposal that Toll-9 might be involved in innate immunity (Ooi et al., 2002). However, a loss-of-function analysis with a defined *Toll-9* null allele did not confirm this prediction (Narbonne-Reveau et al., 2011). Nevertheless, although *Drosophila* Toll-9 does not appear to be directly involved in regulating expression of AMPs, it has been implicated together with a few other Toll-related proteins in cell competition, an organismal surveillance program that monitors cellular fitness and eliminates cells of reduced fitness (losers) (Alpar et al., 2018; Meyer et al., 2014). Depending on the type of cell competition, Toll-9 participates in the expression of the pro-apoptotic genes *reaper* and *hid* in loser cells, triggering their elimination (Alpar et al., 2018; Meyer et al., 2014). Therefore, it has been proposed that the function of Toll signaling for elimination of bacterial pathogens by AMPs and for elimination of unfit cells by pro-apoptotic genes bears a conceptual resemblance between innate immunity and cell competition (Alpar et al., 2018; Meyer et al., 2014).

Apoptosis is an evolutionarily well-conserved process of cellular suicide mediated by a highly specialized class of Cysproteases, termed caspases (reviewed by Fuchs and Steller, 2011; Salvesen et al., 2016; Shalini et al., 2015). In *Drosophila*, the pro-apoptotic genes *reaper* and *hid* promote the activation of the initiator caspase Dronc (caspase-9 homolog in *Drosophila*). Dronc activates the effector caspases DrICE and Dcp-1 (caspase-3 and caspase-7 homologs), which trigger the death of the cell (reviewed in Salvesen et al., 2016; Shalini et al., 2015). However, caspases not only induce apoptosis but can also have non-apoptotic functions (reviewed by Aram et al., 2017; Baena-Lopez, 2018) such as apoptosis-induced proliferation (AiP), during which caspases in apoptotic cells promote the proliferation of surviving cells independently of their role in apoptosis (Diwanji and Bergmann, 2019; Fogarty and Bergmann, 2017).

Early work has shown that AiP requires the initiator caspase Dronc (Fan et al., 2014; Huh et al., 2004; Kondo et al., 2006; Wells et al., 2006). To reveal the mechanism of AiP, we are expressing the pro-apoptotic gene *hid* and the apoptosis inhibitor *p35* simultaneously using

the *ey-Gal4* driver (referred to as *ey > hid,p35*) which drives expression in the larval eye disc anterior to the morphogenetic furrow (MF) (Fan et al., 2014). *p35* encodes a specific inhibitor of the effector caspases DrICE and Dcp-1 but does not block the activity of Dronc (Hawkins et al., 2000; Meier et al., 2000; Yoo et al., 2002). In *ey > hid,p35*-expressing discs, the apoptotic pathway is activated by *hid* expression but blocked downstream because of DrICE and Dcp-1 inhibition by P35, rendering cells in an "undead" condition. Although apoptosis is inhibited in undead tissue, AiP still occurs because of non-apoptotic signaling by the initiator caspase Dronc, triggering hyperplasia of the anterior portion of the larval eye imaginal discs at the expense of the posterior eye field, which is reduced in size (Fan et al., 2014). Combined, these effects result in overgrowth of the adult head capsule (Figure 1B), but a reduction or even absence of the eyes in the adult animal (Fan et al., 2014).

Using the undead model, we showed that AiP is mediated by extracellular reactive oxygen species (ROS) generated by the NADPH oxidase Duox (Fogarty et al., 2016). ROS trigger the recruitment of hemocytes, *Drosophila* immune cells most similar to mammalian macrophages, to undead imaginal discs (Diwanji and Bergmann, 2020). Hemocytes in turn release signals that stimulate JNK activity in undead cells, which then promotes AiP (Fogarty et al., 2016). In addition, JNK can also induce the expression of *hid* (Moreno et al., 2002), thus setting up an amplification loop in undead cells which continuously signals for AiP (Fogarty et al., 2016).

Given that undead cells are abnormal cells (Martin et al., 2009) with potentially altered cellular fitness and that signaling by Toll-related proteins surveilles cellular fitness (Alpar et al., 2018; Meyer et al., 2014), we examined if signaling by Toll-9 has an important function for undead AiP. Here, we show that *Toll-9* is strongly up-regulated in undead cells and is necessary for the overgrowth of undead tissue. Overexpression of *Toll-9* with *p35* induces all hallmarks of undead AiP signaling, including Duox-dependent ROS generation, hemocyte recruitment and JNK signaling. Mechanistically, we provide genetic evidence for a heterologous interaction between Toll-9 and Toll-1, which engages the canonical Toll-1 signaling pathway to promote nuclear translocation of the NF-κB-like transcription factor Dorsal, which induces the expression of *reaper* and *hid*. This activity contributes to the establishment of the feedback amplification loop that signals continuously for AiP. In conclusion, although Toll-9 does not appear to have an important function in innate immunity, it appears to be involved in the expression of pro-apoptotic genes such as *reaper* and *hid* in stress situations such as cell competition and undead AiP.

RESULTS

Toll-9 is required for overgrowth of undead tissue

We examined if *Drosophila Toll-9* is involved in undead AiP. Indeed, depletion of *Toll-9* by RNAi suppressed *ey > hid,p35*-induced overgrowth (Figures 1A–1C; quantified in Figure 1E). We also generated a *Toll-9* deletion mutant by imprecise excision of an existing P element insertion, referred to as $Toll\text{-}9^{rv17}$ (Figure S1A). Heterozygosity of $Toll\text{-}9^{rv17}$ suppressed *ey > hid,p35*-induced overgrowth of undead tissue (Figures 1D and 1E). These results suggest that *Toll-9* is required for *ey > hid,p35*-induced AiP. Furthermore, by qRT-PCR, we found that *Toll-9* mRNA levels increased 8- to 10-fold in *ey > hid,p35* undead

tissue compared with control tissue (Figure 1F). This upregulation of *Toll-9* expression is dependent on JNK encoded by the gene *basket* (*bsk*) (Figure 1F).

Toll-9 is required for ROS generation and hemocyte recruitment

To place *Toll-9* into the AiP network, we performed a number of genetic tests in the *ey > hid,p35* genetic background. *Toll-9* RNAi suppressed the ectopic JNK and Wg activity in *ey > hid,p35* background, suggesting that it acts upstream of these genes (Figure S2). Furthermore, *Toll-9* RNAi or $Toll\text{-}9^{rv17}$ heterozygosity strongly suppressed the generation of ROS (Figures 1G–1J; quantified in Figure 1O). The same set of experiments with a different ROS indicator, H_2DCF-DA, gave similar results (Figure S3). In addition, recruitment of hemocytes to undead discs is reduced to levels seen at control discs in response to *Toll-9* RNAi or $Toll\text{-}9^{rv17}$ heterozygosity (Figures 1K–1N; quantified in Figure 1P). We conclude that *Toll-9* is required for ROS generation and the subsequent recruitment of hemocytes to *ey > hid,p35*-expressing discs.

Toll-9 overexpression in *ey > p35* background engages a similar AiP pathway as *ey > hid,p35*

Although *ey > Gal4*-induced expression of *Toll-9* does not induce any visible phenotype (Figures S1B and S1C), co-expression of *Toll-9* with *p35* (*ey > p35,Toll-9*) is sufficient to cause overgrowth of the resulting head cuticle (Figures 2A and 2B; quantified in Figure 2M). It is unknown why overexpression of *Toll-9* can induce overgrowth only in the presence of *p35* (see Discussion), but we have made a similar observation when overexpressing another factor involved in AiP, called Myo1D (Amcheslavsky et al., 2018). Nevertheless, the *ey > p35,Toll-9*-induced overgrowth phenotype gives us an assay to examine the mechanism by which Toll-9 works in the AiP pathway.

The expression of *Toll-9* in *ey > p35* discs is associated with the generation of ROS as well as recruitment of hemocytes (Figures 2C–2F; quantified in Figures 2N and 2O), consistent with the loss of ROS and hemocyte recruitment by *Toll-9* depletion in *ey > hid,p35* background (Figures 1I, 1J, 1M, and 1N). We showed previously that the membrane-bound NADPH oxidase Duox is required for ROS generation in *ey > hid,p35* imaginal discs, while the second NADPH oxidase, Nox, is not (Fogarty et al., 2016). Consistently, *Duox* RNAi, but not *Nox* RNAi, suppressed the head overgrowth, the generation of ROS, and the recruitment of hemocytes in eye imaginal discs of *ey > p35, Toll-9* animals (Figures 2G–2L; quantified in Figures 2M–2O), suggesting that Toll-9's overgrowth-promoting effect through ROS generation by Duox, but not Nox, is required for the recruitment of hemocytes at *ey > p35,Toll-9* imaginal discs.

JNK signaling is known to mediate signaling and overgrowth in undead tissue (Fan et al., 2014; Martin et al., 2009; Ryoo et al., 2004). Consistently, expression of a RNAi transgene targeting JNK (bsk^{RNAi}) suppressed the head overgrowth of *ey > p35,Toll-9* adult animals (Figures S4A–S4C). We also observed an increase of JNK activity in *ey > p35,Toll-9* imaginal discs based on the JNK reporter *TRE-RFP* (Figures S4D–S4G), suggesting that JNK is induced and required for *Toll-9*-induced overgrowth in the *ey > 35* background.

These similarities between *ey > hid,p35* and *ey > p35,Toll-9* imply that overexpression of *Toll-9* in *ey > 35* background engages a similar hyperplasia pathway compared with *ey > hid,p35* animals. However, in *ey > hid,p35* discs, *hid* induces caspase (i.e., Dronc) activity, which is required for AiP (Fan et al., 2014; Huh et al., 2004; Kondo et al., 2006; Wells et al., 2006). Therefore, we examined if *ey > p35,Toll-9* induces caspase activity. For that purpose, we used the cleaved Dcp-1 (cDcp-1) antibody, which is commonly used as a marker of caspase activity in *Drosophila* tissue (Li et al., 2019). Indeed, although there is no significant caspase activity in *ey > Toll-9* discs, there is increased cDcp-1 labeling evident in *ey > p35,Toll-9* imaginal eye discs (Figures 3C–3E; quantified in Figure 3F). Furthermore, depletion of *dronc* by RNAi resulted in strong suppression of *ey > p35,Toll-9*-induced overgrowth (Figures 3A and 3B), suggesting that *Toll-9* overexpression can induce Dronc activity in the presence of *p35*. These data raise the question of how Toll-9 can achieve this activity.

Toll-9 requires the intracellular domain to induce overgrowth

To address this question, we determined first whether Toll-9 mediates this activity in the AiP network through an intracellular signaling pathway or through cell-cell adhesion mediated by the extracellular domain (Anthoney et al., 2018; Keith and Gay, 1990; Ward et al., 2015). We separately expressed intra- and extracellular domains of Toll-9 ($Toll\text{-}9^{INTRA}$ and $Toll\text{-}9^{EXTRA}$, respectively) linked to the signal peptide and transmembrane domain, in *ey > p35* background. Expression of $Toll\text{-}9^{INTRA}$ is sufficient to induce overgrowth of *ey > p35* head capsules, accompanied by ROS generation and hemocyte activation at imaginal discs (Figures 3G, 3I, and 3K; quantified in Figures 3B, 3M, and 3N). In contrast, expression of $Toll\text{-}9^{EXTRA}$ did not trigger these phenotypes (Figures 3H, 3J, and 3L; quantified in Figures 3B, 3M, and 3N). These data suggest that the intracellular but not the extracellular domain of Toll-9 is sufficient for the generation of ROS, hemocyte activation, and overgrowth of *ey > p35,Toll-9*-expressing tissue, most likely by activation of an intracellular signaling pathway.

To explore the possibility that Toll-9 engages an NF-κB-like transcription factor for this overgrowth, we tested the two NF-κB factors involved in Toll-1 signaling in *Drosophila*, Dorsal and Dif (Ip et al., 1993; Meng et al., 1999; Rutschmann et al., 2000; Steward, 1987). Consistently, RNAi targeting either *dorsal* or *Dif* suppressed the overgrowth of *ey > p35,Toll-*9^{INTRA}-expressing animals (Figures 4A–4C; quantified in Figure 4I). Further support for the notion of an intracellular pathway comes from the observation that knockdown of *Myd88* and a mutant of *tube*, known intracellular components acting upstream of Dorsal and Dif in the Toll-1 pathway (Horng and Medzhitov, 2001; Letsou et al., 1991; Tauszig-Delamasure et al., 2002), also suppressed *ey > p35,Toll-*9^{INTRA}-induced overgrowth strongly and moderately, respectively (Figures 4D and 4E; quantified in Figure 4I). RNAi against another gene involved downstream in Toll-1 signaling, *pelle* (Shelton and Wasserman, 1993; Towb et al., 2001), weakly suppressed *ey > p35,Toll-*9^{INTRA} (Figures 4F–4I). Consistently, RNAi targeting the components of the intracellular Toll-1 signaling pathway also suppressed the *ey > hid,p35* overgrowth phenotype (Figure S5A) although *Myd88* and *pelle* are quite weak suppressors.

One function of the intracellular Myd88/Tube/Pelle pathway is to mediate the nuclear translocation of the NF-κB transcription factor Dorsal (Roth et al., 1989; Rushlow et al., 1989; Steward, 1989). Therefore, we examined if misexpression of Toll-9 can trigger nuclear localization of Dorsal in wing imaginal discs using *ptc-Gal4* as a driver. We chose *ptc-Gal4* in these experiments, because the striped expression of *Toll-9* in the *ptc* domain allows side-by-side comparisons between *ptc*-expressing and *ptc*-non-expressing areas. Consistent with the expectation, there is strong nuclear accumulation of Dorsal in the *ptc* domain upon *Toll-9* (*ptc > Toll-9*) misexpression compared with control (Figures 5A and 5B; see also orthogonal sections on top of the panels). Interestingly, while *ptc > Toll-9* is sufficient to trigger nuclear translocation of Dorsal (Figure 5B2), in the presence of *p35* (*ptc > p35,Toll-9*), the expression domain of *ptc* and the domain where Dorsal is nuclear are strongly enlarged (compare Figures 5C2 and 5C4 with Figures 5B2 and 5B4) further supporting the notion that expression of *Toll-9* induces hyperplasia only in the presence of *p35* (see Discussion). Consistently, we also find nuclear Dorsal in *ey > hid,p35*-expressing eye imaginal discs in a *Toll-9*-dependent manner (Figure S6).

To determine if the intracellular Toll-1 pathway is required for the nuclear translocation of Dorsal, we examined if knockdown of *Myd88* can block the nuclear localization of Dorsal. Indeed, depletion of *Myd88* by RNAi resulted in strong loss of nuclear localization of Dorsal (Figure 5D). Combined, these data suggest that Toll-9 overexpression engages the intracellular Toll-1 pathway involving Myd88, Tube, and Pelle for nuclear localization of Dorsal.

Toll-9 laterally interacts with Toll-1 to stimulate nuclear localization of Dorsal

These observations raise the question whether Toll-9 can promote the nuclear localization of Dorsal by directly engaging the Myd88/Tube/Pelle intracellular pathway or whether it laterally interacts with the Toll-1 receptor, which then activates the intracellular pathway for nuclear translocation of Dorsal. To address this question, we examined the effect of *Toll-1* RNAi on the *ey > p35,Toll-9* overgrowth phenotype. As shown in Figure 4G (quantified in Figure 4I), *Toll-1* RNAi is a strong suppressor of *ey > p35,Toll-9*-induced overgrowth. We also observed that the nuclear localization of Dorsal in the *ptc > p35,Toll-9* expression domain is abolished by *Toll-1* RNAi (Figure 5E). These data imply that Toll-9 can directly or indirectly interact with Toll-1 to engage the known intracellular signaling pathway of Toll-1 for nuclear localization of Dorsal. Consistently, overexpression of *Toll-1* in *ey > p35* background triggers strong overgrowth of the head capsule (Figures S5B and S5C).

Interestingly, RNAi targeting *Spätzle-processing enzyme* (*SPE*), which processes and activates the Toll-1 ligand Spätzle (Spz), strongly suppressed both the *ey > p35,Toll-9*^{INTRA} and *ey > hid,p35* overgrowth phenotypes (Figures 4H, 4I, and S5A). Although we do not observe a suppression of the *ey > p35,Toll-9* overgrowth by *spz* RNAi, overexpression of an active form of *spz*, *spz*^{Act}, in *ey > p35* animals induces strong overgrowth of the head capsules (Figures S5D and S5E). These data imply that the Toll-1 ligand Spz may also be involved in undead overgrowth.

Toll-9 induces expression of *reaper* and *hid* in *p35*-expressing tissue

In the models of cell competition in imaginal discs, evidence was provided that Toll-9 contributes to the expression of the pro-apoptotic genes *reaper* (*rpr*) and *hid* (Meyer et al., 2014). Consistently, RNAi targeting *rpr* strongly suppressed *ey > p35,Toll-9*-induced overgrowth (Figures 6A and 6B; quantified in Figure 6D). Furthermore, depletion of *hid* by RNAi also significantly suppressed *ey > p35,Toll-9*-induced overgrowth (Figures 6C and 6D). These observations suggest that *rpr* and *hid* are required for *p35,Toll-9*-induced overgrowth. Furthermore, although *hid* RNAi suppressed the *ey > hid,p35*-induced overgrowth phenotype as expected, *rpr* RNAi as well as an RNAi line targeting the three pro-apoptotic genes *rpr*, *hid*, and *grim* (*miR*[*RHG*]) also suppressed *ey > hid,p35* (Figure S7A), implying that *rpr* also plays a critical role for *ey > hid,p35*-induced overgrowth. This notion is further supported by examining the expression of *rpr* and *hid* in *ey > p35,Toll-9* background using *lacZ* reporter genes (Figures 6E–6H; quantified in Figure 6I). Interestingly, despite the nuclear localization of Dorsal in *ptc > Toll-9* imaginal discs (Figure 5B), it is able to induce the expression of the *rpr* and *hid* reporter transgenes only in the presence of *p35* (Figures 6F, 6H, and 6I). To explain this discrepancy, we reasoned that because Dorsal acts as a concentration-dependent transcription factor during embryonic dorsoventral patterning (Roth et al., 1989; Rushlow et al., 1989; Steward, 1989), *rpr* and *hid* expression requires a certain nuclear concentration of Dorsal, and therefore we quantified the amount of *Toll-9*-induced nuclear Dorsal in the presence and absence of *p35*. This analysis indeed demonstrates that the amount of nuclear Dorsal is increased in the presence of *p35* (Figure S7B) which would be consistent with a concentration-dependent control of *rpr* and *hid* expression by Dorsal. However, it is also possible that another cofactor is required for Dorsal's ability to induce *rpr* and *hid* expression. This cofactor may not be active or nuclear in the absence of *p35*.

Nevertheless, the lack of *rpr* and *hid* induction in *ey > Toll-9* discs also explains why there is little caspase activity in these discs, while *ey > p35,Toll-9* discs have increased caspase activity (Figures 3C–3F) and are dependent on Dronc for overgrowth (Figures 3A and 3B). Furthermore, given that expression of *hid* and *reaper* in the presence of *p35* induces overgrowth (see, e.g., Figure 1B), these observations explain why *ey > p35,Toll-9* animals have overgrown heads.

DISCUSSION

Toll-9 is the most closely related *Drosophila* TLR compared with mammalian TLRs, but a biological function of Toll-9 has not been clearly defined. All mammalian TLRs are involved in innate immunity; therefore, the close homology has led to the prediction that *Drosophila* Toll-9 also participates in innate immunity (Ooi et al., 2002). However, in *Toll-9* mutants, the basal as well as bacterially induced AMP production is not affected, leading to the conclusion that Toll-9 is not involved in innate immunity (Narbonne-Reveau et al., 2011). Nevertheless, instead of eliminating foreign pathogens, previous work has shown that Toll-9 together with several other Toll-related receptors participates in elimination of unfit cells during cell competition (Alpar et al., 2018; Meyer et al., 2014). This is achieved through the expression of the pro-apoptotic gene *rpr*. Here, we demonstrate that Toll-9 has a

similar *rpr*- and *hid*-inducing function during AiP, thereby adding to the database of Toll-9 function.

To identify the mechanism by which Toll-9 participates in AiP, we took advantage of the observation that misexpression of Toll-9 is sufficient to induce overgrowth of *ey > p35* animals. There are multiple aspects of this phenotype that are worth being discussed. First, key for many of the observations presented in this paper is the presence of P35, a very efficient inhibitor of the effector caspases DrICE and Dcp-1. In the absence of P35, overexpression of Toll-9 does not induce any obvious phenotypes in eye discs or adult heads (see, e.g., Figure S1C). The exact reason for this P35 dependence is currently unknown, but it has also been observed upon misexpression of other genes involved in AiP, such as *Myo1D* (Amcheslavsky et al., 2018), *Toll-1*, and Spz^{Act} (this study). The only known function of P35 is to inhibit DrICE and Dcp-1. Therefore, one possible explanation for the P35 dependence is that these caspases cleave and inactivate an as yet unidentified component of the AiP network, possibly to block inappropriate AiP under normal conditions. In the presence of P35, the AiP-blocking activity of DrICE is inhibited and with the addition of an AiP-inducing stimulus such as misexpression of *Toll-9*, AiP is engaged and can trigger tissue overgrowth.

Second, our data show that ectopic *p35,Toll-9* co-expression triggers overgrowth through a similar mechanism as *hid,p35* co-expression. This includes Dronc activation, Duox-generated ROS, hemocyte recruitment, and JNK activation. These similarities allow us to place the function of Toll-9 into the AiP network.

Third, mis-expressed Toll-9 can genetically interact with Toll-1. This interaction results in nuclear translocation of Dorsal and is dependent on Myd88, Tube, and Pelle, all canonical components of the intracellular Toll-1 signaling pathway (Horng and Medzhitov, 2001; Letsou et al., 1991; Shelton and Wasserman, 1993; Tauszig-Delamasure et al., 2002; Towb et al., 2001). Importantly, the nuclear translocation of Dorsal and the *p35,Toll-9*-induced overgrowth is also dependent on Toll-1, suggesting that the activation of the Myd88/Tube/Pelle pathway is directly triggered by Toll-1 and not by Toll-9. Mechanistically, Toll-9 may activate Toll-1 either directly through hetero-dimerization or mediated by additional factors. Future work will be necessary to identify the molecular mechanism of the Toll-9/Toll-1 interaction.

Fourth, the outcome of the Toll-9/Toll-1 interaction is the expression of the pro-apoptotic genes *reaper* and *hid*. Because *Toll-9* expression is strongly up-regulated in undead cells (Figure 1F), these data suggest that Toll-9-induced expression of *reaper* and *hid* in undead cells is setting up an amplification loop (Figure 7). The cause of the strong transcriptional upregulation of *Toll-9* in undead cells is unknown, but it requires JNK activity (Figures 1F and 7). The Toll-9 amplification loop contributes to the strength of undead signaling during AiP and propels the overgrowth of the tissue.

Fifth, another important question is how Toll signaling becomes activated during AiP. Toll-1 is activated by the ligand Spätzle during embryogenesis and the immune response (Morisato and Anderson, 1994; Weber et al., 2003). Spz requires proteolytic processing for activation,

which during the immune response is mediated by the Ser-protease Spätzle-processing enzyme (Jang et al., 2006; Kambris et al., 2006). Consistently, *SPE* RNAi can suppress both the *ey > p35,Toll-9^{INTRA}* and *ey > hid,p35*-induced overgrowth phenotypes (Figures 4H and S5A). In the experiment in Figure 4H, *SPE* RNAi suppressed *ey > p35,Toll-9^{INTRA}*, which lacks the extracellular domain and should be insensitive to a ligand. Thus, the suppression of *ey > p35,Toll-9^{INTRA}* suggests that SPE does not act through Toll-9 but instead on Toll-1. This result is consistent with a recent finding that *Toll-9* RNAi cannot suppress apoptosis induced by a dominant active *SPE* (*SPE^{Act}*) transgene (Alpar et al., 2018). Although we cannot rule out that there is an unknown Toll-9 ligand, Toll-9 may not need to be activated by a ligand. Toll-9 naturally carries an amino acid substitution in the cysteine-rich extracellular domain similar to the gain-of-function *Toll-1^{1}* mutant (Ooi et al., 2002; Schneider et al., 1991). Indeed, Toll-9 behaves as a constitutively active receptor in cell culture assays (Ooi et al., 2002). As TLRs can form homo- and heterodimers (Hu et al., 2004; Zhang et al., 2002), it is possible that the constitutive activity of Toll-9 and the strong transcriptional upregulation of Toll-9 (Figure 1F) together with ligand stimulation of Toll-1 by Spz is sufficient for the activation of the Toll-1/Toll-9 complex. However, it remains unknown how SPE becomes activated during AiP.

With these considerations in mind, the following model for Toll-9 function during undead AiP emerges (Figure 7). The initial stimulus for AiP is the Gal4-induced expression of *hid* and *p35*, which leads to the activation of Dronc. Because of P35, Dronc cannot induce apoptosis but instead activates Duox for generation of ROS (Figure 7). ROS attract hemocytes which release signals for JNK activation in undead cells. JNK signaling directly or indirectly induces *Toll-9* transcription. Up-regulated Toll-9 interacts with Toll-1, and after Spz ligation the Myd88/Tube/Pelle pathway triggers the nuclear accumulation of Dorsal and potentially Dif (Figure 7). These factors transcriptionally induce *reaper* and *hid* expression setting up the feedback amplification loop, which maintains and propels AiP and overgrowth.

One other interesting question to examine in the future will be how the intracellular pathway of Toll-1 signaling including Dorsal and Dif can induce different target genes under different conditions. For dorsoventral patterning of the *Drosophila* embryo, Dorsal induces the expression of *twist* and *snail* (Ip et al., 1992; Jiang et al., 1991; Pan et al., 1991; Thisse et al., 1991). During immune responses in the fat body, it promotes the expression of AMP genes as well as Kennedy pathway genes for the synthesis of phospholipids (Buchon et al., 2014; Martinez et al., 2020), while during cell competition and AiP which occur in larval imaginal discs, pro-apoptotic genes *hid* and *rpr* are induced. One potential answer to this question is that the specificity of Toll-1 signaling may be modified by the interaction with Toll-9. Although this interaction occurs at the plasma membrane, it also might influence the activity in the nucleus. It will also be interesting to examine if Toll-1 can interact with some or all of the other Toll-related receptors in *Drosophila* and how this interaction might influence the specificity of the transcriptional outcome.

Although *Toll-9* in *Drosophila* does not appear to be required for innate immunity, on the basis of its non-essential function to induce AMP production during bacterial infection (Narbonne-Reveau et al., 2011), our work and work by others (Meyer et al., 2014) reveals

that Toll-9 may have a function during stress responses which involves expression of pro-apoptotic genes such as *rpr* and *hid*. That was demonstrated previously for cell competition (Meyer et al., 2014) and now for undead AiP, indicating potential similarities between cell competition and undead AiP. At first, such similarities appear to be at odds with the common dogmas that proliferating winner cells trigger apoptosis of loser cells, while during AiP, apoptotic cells induce proliferation of surviving cells. However, it has also been reported that loser cells have a much more active role during cell competition and can promote the winner status of cells with increased fitness (Kucinski et al., 2017). Therefore, there appear to be significant similarities between cell competition and undead AiP. The common denominator for both systems is the expression of pro-apoptotic genes. These responses have different outcomes in both systems. During cell competition, this response involves the death of the loser cells (Alpar et al., 2018; Meyer et al., 2014). During undead AiP, it sets up the amplification loop known to operate in undead cells (Fogarty et al., 2016), which propels hyperplasia and tissue overgrowth.

Limitations of the study

This work was performed largely under undead conditions (i.e., in the presence of the effector caspase inhibitor p35, which is not an endogenous gene in *Drosophila*). In reality, however, in the absence of p35, effector caspases are also activated in apoptotic cells, which will eventually lead to the death of the cell. Therefore, the question arises as to how apoptosis and AiP are linked to allow compensatory proliferation under normal conditions. Recently, we presented evidence that certain apoptotic cells (dying enterocytes in the adult intestine) can adopt a transiently undead-like state that enables them to signal for AiP before they are dying and removed (Amcheslavsky et al., 2020). The transiently undead-like state is achieved by transient localization of Dronc to the plasma membrane, which might serve as a non-apoptotic compartment of the cell (Amcheslavsky et al., 2018; Bergmann, 2018). In that way, apoptotic cells, before they die, can trigger AiP in a p35-independent manner. Therefore, in future research, it will be important to examine if the Toll-9/Toll-1 interaction sets up a similar amplification loop in transiently undead enterocytes.

STAR★METHODS

RESOURCE AVAILABILITY

Lead contact—Further information and requests for resources and reagents should be directed to and will be fulfilled by the lead contact, Andreas Bergmann (andreas.bergmann@umassmed.edu).

Materials availability—All unique/stable materials generated in this study is available from the lead contact without restriction.

Data and code availability—All data reported in this paper will be shared by the lead contact upon request. This study does not report original code. Any additional information required to reanalyze the data reported in this paper is available from the lead contact upon request.

EXPERIMENTAL MODEL AND SUBJECT DETAILS

The experimental model organism is *Drosophila melanogaster*. Details of genotypes used in this study and their sources are described in the key resources table (KRT). All crosses were performed on standard cornmeal-molasses medium (60g/L cornmeal, 60mL/L molasses, 23.5g/L bakers yeast, 6.5g/L agar, 4mL/L acid mix and 0.13% Tegosept). For expression of RNAi transgenes and mis-expressing transgenes in eye and wing imaginal discs the Gal4/UAS system was used. Crosses not involving conditional expression of transgenes were incubated at 25°C.

METHOD DETAILS

Fly stocks and genetics—The exact genotype of *ey > hid,p35* is *UAS-hid* (on X); *ey-Gal4 UAS-p35* (on 2nd) and of *ey > p35* it is *ey-Gal4 UAS-p35* (on 2nd).

The following fly stocks were used: *ey > hid,p35* and *ey > p35* (Fan et al., 2014); *UAS-Nox* RNAi (line#4) and *UAS-Duox* RNAi (#44) (Ha et al., 2005; Tanji et al., 2010); $Toll\text{-}9^{rv17}$, *UAS-Toll-9*, $UAS\text{-}Toll\text{-}9^{INTRA}$ and $UAS\text{-}Toll\text{-}9^{EXTRA}$ (this study); *UAS-Toll-9* RNAi stocks: BL30535, v36308 and v109635; *UAS-Dif* RNAi: v100537; *UAS-dl* RNAi: BL34938 and v105491; *UAS-Myd88* RNAi: v106198; $tube^{3}$ mutant (Letsou et al., 1991); *UAS-pelle* RNAi: v103774; *UAS-Toll-1* RNAi: v100078; *UAS-rpr* RNAi: BL51846; *UAS-hid* RNAi: v7912, *UAS-dronc* RNAi: v100424; *UAS-bsk* RNAi (v34138); *UAS-Lucif-erase* RNAi: BL31603 (used as the mock RNAi); 4kb *rpr-lacZ* (Jiang et al., 2000); *hid[10–1kb]-lacZ* (line1) (this work); *TRE-RFP* (Chatterjee and Bohmann, 2012); *UAS-SPE* RNAi: v104906; *UAS-Toll-1* (Hu et al., 2004); $UAS\text{-}spz^{Act}$ (Ligoxygakis et al., 2002).

Generation of the $Toll\text{-}9^{rv17}$ allele—The parental P element insertion strain EY14405 from Bloomington stock center was used for a jump out excision screen. The strain was crossed with a Δ2–3 strain and offspring with loss of red eye color were collected. Individual flies collected were crossed with balancer strain to establish individual stocks. Genomic DNA from these collected stocks were isolated and tested by PCR using primers surrounding the P element insertion site. The *revertant 17* (*rv17*) stock showed absence of PCR product on primary screen and the homozygous strain were subject to further PCR and sequencing to confirm the deletion of the *Toll-9* locus, from the insertion site in the second intron to the last coding exon as shown in Figure S1A.

Generation of $UAS\text{-}Toll\text{-}9^{INTRA}$ and $UAS\text{-}Toll\text{-}9^{EXTRA}$—For $UAS\text{-}Toll\text{-}9^{EXTRA}$, the *Toll-9* cDNA was used to PCR amplify the first part of the coding sequence, from 5′ UTR to the beginning of cytoplasmic domain including the transmembrane domain. The clone encodes a.a. 1 to 700. The PCR fragment was cloned into the XbaI and BglII sites of the pUAST vector. For $UAS\text{-}Toll\text{-}9^{INTRA}$, the *Toll-9* cDNA was used to amplify a short fragment encoding the first 15 a.a., as signal peptide sequence, and a second fragment encoding a.a. 650, to the stop codon, including the transmembrane and the cytoplasmic domains. The two fragments were cloned head to tail into the XbaI and BglII sites of the pUAST vector. The resulting plasmids were used to generate transgenic flies (Rainbow Transgene, California) in the w^{1118} background. The resulting transgenic flies were used for crosses into the *ey > p35* background.

Generation of *hid[10-1kb]-lacZ*—The 10 kb genomic DNA upstream of the *hid* transcriptional start site was cloned and inserted into a *Drosophila* reporter plasmid, pCaSpeR-hs43 lacZ. Transgenic flies were then generated using standard procedures. The *hid[10-1]-lacZ* reporter was found to respond to Toll-9 signaling and was used in this study as the *hid* reporter.

Immunolabeling and ROS staining—For labelings with antibodies, fixed eye-antennal or wing imaginal discs from 3rd instar larvae were used following standard protocols (Fogarty et al., 2016). The monoclonal NimC antibody is a kind gift of István Andó (Kurucz et al., 2007) and was used at a dilution of 1:300. Primary antibodies from the Developmental Studies Hybridoma Bank (DSHB) included anti-Dorsal (7A4) used at 1:20, anti-Mmp1 (3A6B4) used at 1:50, anti-Wingless (4D4) used at 1:50, anti-beta-galactosidase (40–1a) used at 1:20, and anti-Elav (7E8A10) used at 1:50. Anti-cDcp1 (Asp216) antibody from Cell Signaling Technology was used at 1:200. Hoechst 33342 solution was used at 1:1000 to stain nuclei. Fluorescent secondary antibodies were obtained from Jackson ImmunoResearch. ROS staining with DHE (Invitrogen #D23107) and H_2DCF-DA (Molecular Probes #C6827) were performed on unfixed imaginal discs using published protocols (Owusu-Ansah et al., 2008).

qRT-PCR for determination of *Toll-9* transcript levels—Total mRNA was prepared from eye-imaginal discs using TRIzol reagent (Ambion, Cat#15596026). cDNA was prepared using QuantiTect Reverse Transcription Kit (Qiagen, Cat# 205311) and qPCR was performed with Power SYBR Green PCR master mix (Applied Biosystems, Cat#4367659). The following primer pairs were used:

Toll-9, Forward: 5′-CCATTACAAGCACTATAGG; Reverse: 5′-GACCTCTTCGGCCTCTTC.

RP-49: Forward: 5′-CCAGTCGGATCGATATGCTAA; Reverse: 5′-ACGTTGTGCACCAGGAACTT.

QUANTIFICATION AND STATISTICAL ANALYSIS

For quantification of confocal images, the ‘Histo’ function of Zen (2012) imaging software (Carl Zeiss) was used. Region of interest was outlined for each disc and mean fluorescence signal intensity was determined. Crosses were repeated at least three times. Analysis and graph generation was done using GraphPad Prism 9. The statistical method used was one-way ANOVA with Holm-Sidak test for multiple comparisons, unless otherwise indicated. Plotted is mean intensity ±SEM. Levels of significance are depicted by asterisks in the figures: *$p < 0.05$; **$p < 0.01$; ***$p < 0.001$; ****$p < 0.0001$.

N numbers are as follows:

Figure 1O: 4, 8, 4, 7 (from left to right)

Figure 1P: 5, 6, 6, 5 (from left to right)

Figure 2N: 4, 4, 6, 6 (from left to right)

Figure 2O: 7, 12, 7, 6 (from left to right)

Figure 3F: 7, 9, 12 (from left to right)

Figure 3M: 4, 4, 6, 7 (from left to right)

Figure 3N: 5, 11, 10, 4 (from left to right)

Figure 6I: 7, 15, 4, 17 (from left to right)

Figure S3F: 3, 6, 5, 6, 7 (from left to right)

Figure S4G: 8, 9, 11 (from left to right)

Figure S7B: 50, 50 (from left to right)

Supplementary Material

Refer to Web version on PubMed Central for supplementary material.

ACKNOWLEDGMENTS

We would like to thank István Andó, Dirk Bohmann, Laura Johnston, Won Jae Lee, Julien Royet, the Bloomington *Drosophila* Stock Center, and the Vienna *Drosophila* Resource Center for fly stocks. This work was funded by the National Institute of General Medical Sciences under award R35GM118330 to A.B. YTI was supported by NIH grants GM107457 and DK083450. The content is solely the responsibility of the authors and does not necessarily represent the official views of the NIH. Y.T.I. is a member of the UMass Center for Clinical and Translational Science (UL1TR000161).

REFERENCES

Akhouayri I, Turc C, Royet J, and Charroux B (2011). Toll-8/Tollo negatively regulates antimicrobial response in the Drosophila respiratory epithelium. PLoS Pathog. 7, e1002319. 10.1371/journal.ppat.1002319. [PubMed: 22022271]

Alpar L, Bergantinos C, and Johnston LA (2018). Spatially restricted regulation of spatzle/toll signaling during cell competition. Dev. Cell 46, 706–719.e5. 10.1016/j.devcel.2018.08.001. [PubMed: 30146479]

Amcheslavsky A, Lindblad JL, and Bergmann A (2020). Transiently “undead” enterocytes mediate homeostatic tissue turnover in the adult Drosophila midgut. Cell Rep. 33, 108408. 10.1016/j.celrep.2020.108408. [PubMed: 33238125]

Amcheslavsky A, Wang S, Fogarty CE, Lindblad JL, Fan Y, and Bergmann A (2018). Plasma membrane localization of apoptotic caspases for non-apoptotic functions. Dev. Cell 45, 450–464.e3. 10.1016/j.devcel.2018.04.020. [PubMed: 29787709]

Anderson KV, Bokla L, and Nusslein-Volhard C (1985a). Establishment of dorsal-ventral polarity in the Drosophila embryo: the induction of polarity by the Toll gene product. Cell 42, 791–798. 10.1016/0092-8674(85)90275-2. [PubMed: 3931919]

Anderson KV, Jurgens G, and Nusslein-Volhard C (1985b). Establishment of dorsal-ventral polarity in the Drosophila embryo: genetic studies on the role of the Toll gene product. Cell 42, 779–789. 10.1016/0092-8674(85)90274-0. [PubMed: 3931918]

Anthoney N, Foldi I, and Hidalgo A (2018). Toll and Toll-like receptor signalling in development. Development 145, dev156018. [PubMed: 29695493]

Aram L, Yacobi-Sharon K, and Arama E (2017). CDPs: caspase-dependent non-lethal cellular processes. Cell Death Differ. 24, 1307–1310. 10.1038/cdd.2017.111. [PubMed: 28695898]

Baena-Lopez LA (2018). All about the caspase-dependent functions without cell death. Semin. Cell Dev. Biol. 82, 77–78. 10.1016/j.semcdb.2018.01.005. [PubMed: 29339195]

Benton MA, Pechmann M, Frey N, Stappert D, Conrads KH, Chen YT, Stamataki E, Pavlopoulos A, and Roth S (2016). Toll genes have an ancestral role in Axis elongation. Curr. Biol. 26, 1609–1615. 10.1016/j.cub.2016.04.055. [PubMed: 27212406]

Bergmann A (2018). Are membranes non-apoptotic compartments for apoptotic caspases? Oncotarget 9, 31566–31567. 10.18632/oncotarget.25796. [PubMed: 30167077]

Bettencourt R, Tanji T, Yagi Y, and Ip YT (2004). Toll and Toll-9 in Drosophila innate immune response. J. Endotoxin Res. 10, 261–268. 10.1177/09680519040100040101. [PubMed: 15373972]

Bilak H, Tauszig-Delamasure S, and Imler JL (2003). Toll and toll-like receptors in Drosophila. Biochem. Soc. Trans. 31, 648–651. 10.1042/bst0310648. [PubMed: 12773174]

Buchon N, Silverman N, and Cherry S (2014). Immunity in Drosophila melanogaster–from microbial recognition to whole-organism physiology. Nat. Rev. Immunol. 14, 796–810. 10.1038/nri3763. [PubMed: 25421701]

Chatterjee N, and Bohmann D (2012). A Versatile FC31 based reporter system for measuring AP-1 and Nrf2 signaling in Drosophila and in tissue culture. PLoS One 7, e34063. 10.1371/journal.pone.0034063. [PubMed: 22509270]

Diwanji N, and Bergmann A (2019). Two sides of the same coin - compensatory proliferation in regeneration and cancer. Adv. Exp. Med. Biol. 1167, 65–85. 10.1007/978-3-030-23629-8_4. [PubMed: 31520349]

Diwanji N, and Bergmann A (2020). Basement membrane damage by ROS- and JNK-mediated Mmp2 activation drives macrophage recruitment to overgrown tissue. Nat. Commun. 11, 3631. 10.1038/s41467-020-17399-8. [PubMed: 32686670]

Fan Y, Wang S, Hernandez J, Yenigun VB, Hertlein G, Fogarty CE, Lindblad JL, and Bergmann A (2014). Genetic models of apoptosis-induced proliferation decipher activation of JNK and identify a requirement of EGFR signaling for tissue regenerative responses in Drosophila. PLoS Genet. 10, e1004131. 10.1371/journal.pgen.1004131. [PubMed: 24497843]

Fogarty CE, and Bergmann A (2017). Killers creating new life: caspases drive apoptosis-induced proliferation in tissue repair and disease. Cell Death Differ. 24, 1390–1400. 10.1038/cdd.2017.47. [PubMed: 28362431]

Fogarty CE, Diwanji N, Lindblad JL, Tare M, Amcheslavsky A, Makhijani K, Bruckner K, Fan Y, and Bergmann A (2016). Extracellular reactive oxygen species drive apoptosis-induced proliferation via Drosophila macrophages. Curr. Biol. 26, 575–584. 10.1016/j.cub.2015.12.064. [PubMed: 26898463]

Fuchs Y, and Steller H (2011). Programmed cell death in animal development and disease. Cell 147, 742–758. 10.1016/j.cell.2011.10.033. [PubMed: 22078876]

Ha EM, Oh CT, Bae YS, and Lee WJ (2005). A direct role for dual oxidase in Drosophila gut immunity. Science 310, 847–850. 10.1126/science.1117311. [PubMed: 16272120]

Hawkins CJ, Yoo SJ, Peterson EP, Wang SL, Vernooy SY, and Hay BA (2000). The Drosophila caspase DRONC cleaves following glutamate or aspartate and is regulated by DIAP1, HID, and GRIM. J. Biol. Chem. 275, 27084–27093. 10.1016/s0021-9258(19)61483-3. [PubMed: 10825159]

Horng T, and Medzhitov R (2001). Drosophila MyD88 is an adapter in the Toll signaling pathway. Proc. Natl. Acad. Sci. U S A 98, 12654–12658. 10.1073/pnas.231471798. [PubMed: 11606776]

Hu X, Yagi Y, Tanji T, Zhou S, and Ip YT (2004). Multimerization and interaction of toll and spatzle in Drosophila. Proc. Natl. Acad. Sci. U S A 101, 9369–9374. 10.1073/pnas.0307062101. [PubMed: 15197269]

Huh JR, Guo M, and Hay BA (2004). Compensatory proliferation induced by cell death in the Drosophila wing disc requires activity of the apical cell death caspase Dronc in a nonapoptotic role. Curr. Biol. 14, 1262–1266. 10.1016/j.cub.2004.06.015. [PubMed: 15268856]

Ip YT, Park RE, Kosman D, Yazdanbakhsh K, and Levine M (1992). dorsal-twist interactions establish snail expression in the presumptive mesoderm of the Drosophila embryo. Genes Dev. 6, 1518–1530. 10.1101/gad.6.8.1518. [PubMed: 1644293]

Ip YT, Reach M, Engstrom Y, Kadalayil L, Cai H, Gonzalez-Crespo S, Tatei K, and Levine M (1993). Dif, a dorsal-related gene that mediates an immune response in Drosophila. Cell 75, 753–763. 10.1016/0092-8674(93)90495-c. [PubMed: 8242747]

Jang IH, Chosa N, Kim SH, Nam HJ, Lemaitre B, Ochiai M, Kambris Z, Brun S, Hashimoto C, Ashida M, et al. (2006). A Spatzle-processing enzyme required for toll signaling activation in Drosophila innate immunity. Dev. Cell 10, 45–55. 10.1016/j.devcel.2005.11.013. [PubMed: 16399077]

Jiang C, Lamblin AFJ, Steller H, and Thummel CS (2000). A steroid-triggered transcriptional hierarchy controls salivary gland cell death during Drosophila metamorphosis. Mol. Cell 5, 445–455. 10.1016/s1097-2765(00)80439-6. [PubMed: 10882130]

Jiang J, Kosman D, Ip YT, and Levine M (1991). The dorsal morphogen gradient regulates the mesoderm determinant twist in early Drosophila embryos. Genes Dev. 5, 1881–1891. 10.1101/gad.5.10.1881. [PubMed: 1655572]

Kambris Z, Brun S, Jang IH, Nam HJ, Romeo Y, Takahashi K, Lee WJ, Ueda R, and Lemaitre B (2006). Drosophila immunity: a large-scale in vivo RNAi screen identifies five serine proteases required for Toll activation. Curr. Biol. 16, 808–813. 10.1016/j.cub.2006.03.020. [PubMed: 16631589]

Keith FJ, and Gay NJ (1990). The Drosophila membrane receptor Toll can function to promote cellular adhesion. EMBO J. 9, 4299–4306. 10.1002/j.1460-2075.1990.tb07878.x. [PubMed: 2124970]

Khush RS, and Lemaitre B (2000). Genes that fight infection: what the Drosophila genome says about animal immunity. Trends Genet. 16, 442–449. 10.1016/s0168-9525(00)02095-3. [PubMed: 11050330]

Kondo S, Senoo-Matsuda N, Hiromi Y, and Miura M (2006). DRONC coordinates cell death and compensatory proliferation. Mol. Cell Biol. 26, 7258–7268. 10.1128/mcb.00183-06. [PubMed: 16980627]

Kucinski I, Dinan M, Kolahgar G, and Piddini E (2017). Chronic activation of JNK JAK/STAT and oxidative stress signalling causes the loser cell status. Nat. Commun. 8, 136. 10.1038/s41467-017-00145-y. [PubMed: 28743877]

Kurucz E, Vaczi B, Markus R, Laurinyecz B, Vilmos P, Zsamboki J, Csorba K, Gateff E, Hultmark D, and Ando I (2007). Definition of Drosophila hemocyte subsets by cell-type specific antigens. Acta Biol. Hung. 58, 95–111. 10.1556/abiol.58.2007.suppl.8. [PubMed: 18297797]

Lamiable O, Arnold J, de Faria I, Olmo RP, Bergami F, Meignin C, Hoffmann JA, Marques JT, and Imler JL (2016). Analysis of the contribution of hemocytes and autophagy to Drosophila antiviral immunity. J. Virol. 90, 5415–5426. 10.1128/jvi.00238-16. [PubMed: 27009948]

Lemaitre B (2004). The road to Toll. Nat. Rev. Immunol. 4, 521–527. 10.1038/nri1390. [PubMed: 15229471]

Lemaitre B, Nicolas E, Michaut L, Reichhart JM, and Hoffmann JA (1996). The dorsoventral regulatory gene cassette spatzle/Toll/cactus controls the potent antifungal response in Drosophila adults. Cell 86, 973–983. 10.1016/s0092-8674(00)80172-5. [PubMed: 8808632]

Letsou A, Alexander S, Orth K, and Wasserman SA (1991). Genetic and molecular characterization of tube, a Drosophila gene maternally required for embryonic dorsoventral polarity. Proc. Natl. Acad. Sci. U S A 88, 810–814. 10.1073/pnas.88.3.810. [PubMed: 1899484]

Li M, Sun S, Priest J, Bi X, and Fan Y (2019). Characterization of TNF-induced cell death in Drosophila reveals caspase- and JNK-dependent necrosis and its role in tumor suppression. Cell Death Dis. 10, 613. 10.1038/s41419-019-1862-0. [PubMed: 31409797]

Ligoxygakis P, Pelte N, Hoffmann JA, and Reichhart JM (2002). Activation of Drosophila Toll during fungal infection by a blood serine protease. Science 297, 114–116. 10.1126/science.1072391. [PubMed: 12098703]

Martin FA, Perez-Garijo A, and Morata G (2009). Apoptosis in Drosophila: compensatory proliferation and undead cells. Int. J. Dev. Biol. 53, 1341–1347. 10.1387/ijdb.072447fm. [PubMed: 19247932]

Martinez BA, Hoyle RG, Yeudall S, Granade ME, Harris TE, Castle JD, Leitinger N, and Bland ML (2020). Innate immune signaling in Drosophila shifts anabolic lipid metabolism from triglyceride storage to phospholipid synthesis to support immune function. PLoS Genet. 16, e1009192. 10.1371/journal.pgen.1009192. [PubMed: 33227003]

Meier P, Silke J, Leevers SJ, and Evan GI (2000). The Drosophila caspase DRONC is regulated by DIAP1. EMBO J. 19, 598–611. 10.1093/emboj/19.4.598. [PubMed: 10675329]

Meng X, Khanuja BS, and Ip YT (1999). Toll receptor-mediated Drosophila immune response requires Dif, an NF-kappa B factor. Genes Dev. 13, 792–797. 10.1101/gad.13.7.792. [PubMed: 10197979]

Meyer SN, Amoyel M, Bergantinos C, de la Cova C, Schertel C, Basler K, and Johnston LA (2014). An ancient defense system eliminates unfit cells from developing tissues during cell competition. Science 346, 1258236. 10.1126/science.1258236. [PubMed: 25477468]

Moreno E, Yan M, and Basler K (2002). Evolution of TNF signaling mechanisms. Curr. Biol. 12, 1263–1268. 10.1016/s0960-9822(02)00954-5. [PubMed: 12176339]

Morisato D, and Anderson KV (1994). The spatzle gene encodes a component of the extracellular signaling pathway establishing the dorsal-ventral pattern of the Drosophila embryo. Cell 76, 677–688. 10.1016/0092-8674(94)90507-x. [PubMed: 8124709]

Nakamoto M, Moy RH, Xu J, Bambina S, Yasunaga A, Shelly SS, Gold B, and Cherry S (2012). Virus recognition by Toll-7 activates antiviral autophagy in Drosophila. Immunity 36, 658–667. 10.1016/j.immuni.2012.03.003. [PubMed: 22464169]

Narbonne-Reveau K, Charroux B, and Royet J (2011). Lack of an antibacterial response defect in Drosophila Toll-9 mutant. PLoS One 6, e17470. 10.1371/journal.pone.0017470. [PubMed: 21386906]

Nusslein-Volhard C (2021). The Toll gene in Drosophila pattern formation. Trends Genet. 38, 231–245. [PubMed: 34649739]

Ooi JY, Yagi Y, Hu X, and Ip YT (2002). The Drosophila Toll-9 activates a constitutive antimicrobial defense. EMBO Rep. 3, 82–87. 10.1093/embo-reports/kvf004. [PubMed: 11751574]

Owusu-Ansah E, Yavari A, and Banerjee U (2008). A protocol for in vivo detection of reactive oxygen species. Nat. Protoc. Exchange. 10.1038/nprot.2008.23.

Pan DJ, Huang JD, and Courey AJ (1991). Functional analysis of the Drosophila twist promoter reveals a dorsal-binding ventral activator region. Genes Dev. 5, 1892–1901. 10.1101/gad.5.10.1892. [PubMed: 1655573]

Pare AC, Vichas A, Fincher CT, Mirman Z, Farrell DL, Mainieri A, and Zallen JA (2014). A positional Toll receptor code directs convergent extension in Drosophila. Nature 515, 523–527. 10.1038/nature13953. [PubMed: 25363762]

Roth S, Stein D, and Nusslein-Volhard C (1989). A gradient of nuclear localization of the dorsal protein determines dorsoventral pattern in the Drosophila embryo. Cell 59, 1189–1202. 10.1016/0092-8674(89)90774-5. [PubMed: 2688897]

Rushlow CA, Han K, Manley JL, and Levine M (1989). The graded distribution of the dorsal morphogen is initiated by selective nuclear transport in Drosophila. Cell 59, 1165–1177. 10.1016/0092-8674(89)90772-1. [PubMed: 2598265]

Rutschmann S, Jung AC, Hetru C, Reichhart JM, Hoffmann JA, and Ferrandon D (2000). The Rel protein DIF mediates the antifungal but not the antibacterial host defense in Drosophila. Immunity 12, 569–580. 10.1016/s1074-7613(00)80208-3. [PubMed: 10843389]

Ryoo HD, Gorenc T, and Steller H (2004). Apoptotic cells can induce compensatory cell proliferation through the JNK and the Wingless signaling pathways. Dev. Cell 7, 491–501. 10.1016/j.devcel.2004.08.019. [PubMed: 15469838]

Salvesen GS, Hempel A, and Coll NS (2016). Protease signaling in animal and plant-regulated cell death. FEBS J. 283, 2577–2598. 10.1111/febs.13616. [PubMed: 26648190]

Schneider DS, Hudson KL, Lin TY, and Anderson KV (1991). Dominant and recessive mutations define functional domains of Toll, a transmembrane protein required for dorsal-ventral polarity in the Drosophila embryo. Genes Dev. 5, 797–807. 10.1101/gad.5.5.797. [PubMed: 1827421]

Shalini S, Dorstyn L, Dawar S, and Kumar S (2015). Old, new and emerging functions of caspases. Cell Death Differ. 22, 526–539. 10.1038/cdd.2014.216. [PubMed: 25526085]

Shelton CA, and Wasserman SA (1993). Pelle encodes a protein kinase required to establish dorsoventral polarity in the Drosophila embryo. Cell 72, 515–525. 10.1016/0092-8674(93)90071-w. [PubMed: 8440018]

Steward R (1987). *Dorsal*, an embryonic polarity gene in *Drosophila*, is homologous to the Vertebrate proto-oncogene, c- rel. Science 238, 692–694. 10.1126/science.3118464. [PubMed: 3118464]

Steward R (1989). Relocalization of the dorsal protein from the cytoplasm to the nucleus correlates with its function. Cell 59, 1179–1188. 10.1016/0092-8674(89)90773-3. [PubMed: 2598266]

Tanji T, Yun EY, and Ip YT (2010). Heterodimers of NF-κB transcription factors DIF and Relish regulate antimicrobial peptide genes in *Drosophila*. Proc. Natl. Acad. Sci. U S A 107, 14715–14720. 10.1073/pnas.1009473107. [PubMed: 20679214]

Tauszig-Delamasure S, Bilak H, Capovilla M, Hoffmann JA, and Imler JL (2002). Drosophila MyD88 is required for the response to fungal and Gram-positive bacterial infections. Nat. Immunol. 3, 91–97. 10.1038/ni747. [PubMed: 11743586]

Tauszig S, Jouanguy E, Hoffmann JA, and Imler JL (2000). Toll-related receptors and the control of antimicrobial peptide expression in Drosophila. Proc. Natl. Acad. Sci. U S A 97, 10520–10525. 10.1073/pnas.180130797. [PubMed: 10973475]

Thisse C, Perrin-Schmitt F, Stoetzel C, and Thisse B (1991). Sequence-specific transactivation of the Drosophila twist gene by the dorsal gene product. Cell 65, 1191–1201. 10.1016/0092-8674(91)90014-p. [PubMed: 1648449]

Towb P, Bergmann A, and Wasserman SA (2001). The protein kinase Pelle mediates feedback regulation in the Drosophila Toll signaling pathway. Development 128, 4729–4736. 10.1242/dev.128.23.4729. [PubMed: 11731453]

Ward A, Hong W, Favaloro V, and Luo L (2015). Toll receptors instruct axon and dendrite targeting and participate in synaptic partner matching in a Drosophila olfactory circuit. Neuron 85, 1013–1028. 10.1016/j.neuron.2015.02.003. [PubMed: 25741726]

Wasserman SA (2000). Toll signaling: the enigma variations. Curr. Opin. Genet. Dev. 10, 497–502. 10.1016/s0959-437x(00)00118-0. [PubMed: 10980426]

Weber ANR, Tauszig-Delamasure S, Hoffmann JA, Lelievre E, Gascan H, Ray KP, Morse MA, Imler JL, and Gay NJ (2003). Binding of the Drosophila cytokine Spatzle to Toll is direct and establishes signaling. Nat. Immunol. 4, 794–800. 10.1038/ni955. [PubMed: 12872120]

Wells BS, Yoshida E, and Johnston LA (2006). Compensatory proliferation in Drosophila imaginal discs requires Dronc-dependent p53 activity. Curr. Biol. 16, 1606–1615. 10.1016/j.cub.2006.07.046. [PubMed: 16920621]

Yoo SJ, Huh JR, Muro I, Yu H, Wang L, Wang SL, Feldman RMR, Clem RJ, Müller HAJ, and Hay BA (2002). Hid, Rpr and Grim negatively regulate DIAP1 levels through distinct mechanisms. Nat. Cell Biol. 4, 416–424. 10.1038/ncb793. [PubMed: 12021767]

Zhang H, Tay PN, Cao W, Li W, and Lu J (2002). Integrin-nucleated Toll-like receptor (TLR) dimerization reveals subcellular targeting of TLRs and distinct mechanisms of TLR4 activation and signaling. FEBS Lett. 532, 171–176. 10.1016/s0014-5793(02)03669-4. [PubMed: 12459484]

Highlights

- *Toll-9* is required for undead apoptosis-induced proliferation (AiP)
- Toll-9 interacts with Toll-1 to activate the intracellular Toll-1 pathway
- NF-κB-like transcription factors induce expression of apoptotic genes *reaper* and *hid*
- Toll-9/Toll-1 signaling establishes an amplification loop for AiP

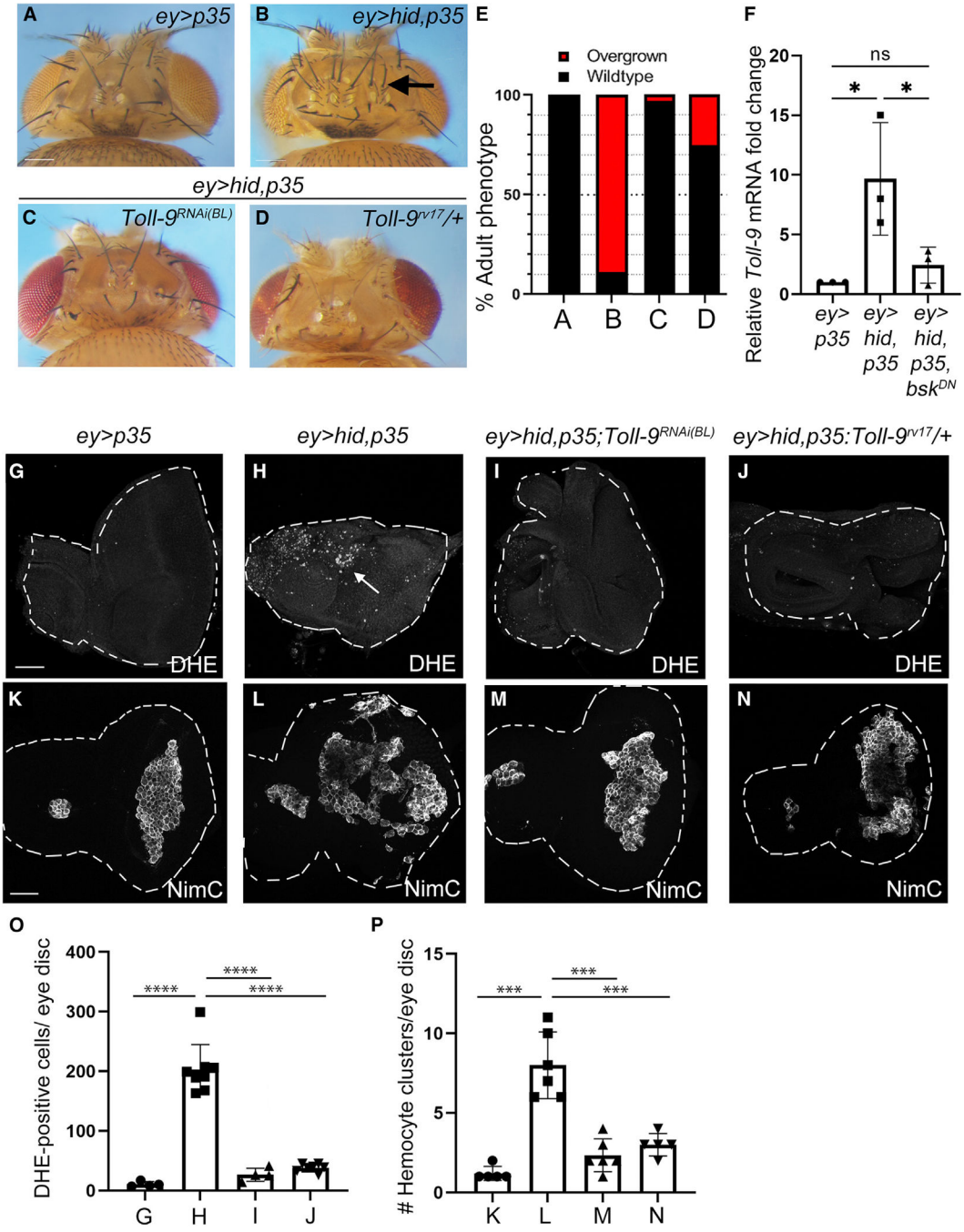

Figure 1. *Toll-9* is required for *ey > hid,p35*-induced overgrowth, ROS generation, and hemocyte activation

(A–D) Reduction of *Toll-9* activity by RNAi (C) or the heterozygous *Toll-9*^{rv17} mutant (D) suppressed *ey > hid,p35*-induced overgrowth (B). Arrow in (B) points to additional bristles and ocelli. Expression of *p35* (*ey > p35*) (A) does not trigger overgrowth. Scale bar: 200 μm. (E) Quantification of the data in (A)–(D). On the basis of qualitative screening criteria, overgrowth of progeny is scored by the presence of additional bristles and ocelli, expansion of the head capsule, and amorphic overgrowth. In severe cases, eye tissue is lost. At least 100 flies were scored for each genotype.

(F) *ey > hid,p35* induces *Toll-9* expression in a JNK (*basket* [*bsk*])-dependent manner. Relative mRNA levels of *Toll-9* in *ey-Gal4*, *ey > hid,p35* and *ey > hid,p35,bsk^{DN}* genetic backgrounds. The average of three independent experiments is plotted using one-way ANOVA with the Holm-Sidak test for multiple comparisons. *p < 0.05. Plotted is the mean intensity ± SEM. ns, not significant.

(G–N) ROS generation (G–J) and hemocyte recruitment (K–N) in *ey > hid,p35* eye imaginal discs are strongly reduced by *Toll-9* RNAi and the heterozygous *Toll-9^{rv17}* mutant. Dihydroethidium (DHE) was used as ROS indicator. Arrow in (H) highlights DHE labeling. Anti-NimC antibody was used as hemocyte marker. Scale bars: 50 μm.

(O and P) Quantification of the data in (G)–(J) and (K)–(N), respectively. DHE counts and number of hemocyte clusters were counted across entire discs. Data were analyzed using one-way ANOVA with the Holm-Sidak test for multiple comparisons. Plotted is the mean ± SEM. ***p < 0.001 and ****p < 0.0001.

The following numbers of discs were analyzed: 4 (G), 8 (H), 4 (I), 7 (J), 5 (K), 6 (L), 6 (M), and 5 (N). The *Toll-9$^{RNAi(BL)}$* line in (B), (I), and (M) is Bloomington stock #BL35035. See also Figures S1–S4.

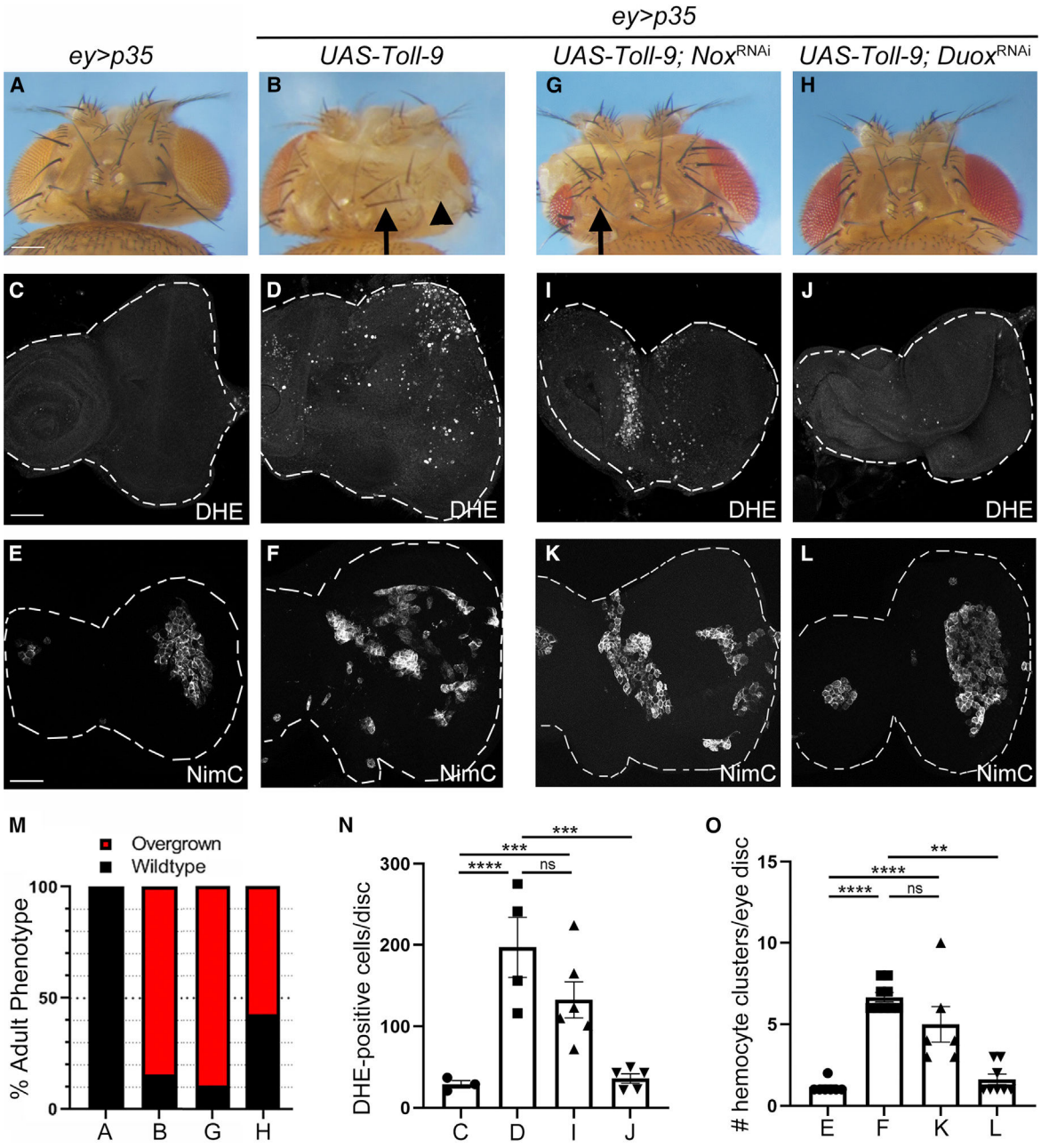

Figure 2. Toll-9 promotes overgrowth of *ey > p35* head capsules and hemocyte recruitment via Duox-generated ROS

(A and B) Transgenic expression of *Toll-9* causes overgrowth of the head capsule of *ey > p35*-animals. Quantified in (M). The arrow in (B) highlights additional bristles, the arrowhead overgrown cuticle at the expense of eye tissue. Scale bar: 200 μm.

(C–F) Transgenic expression of *Toll-9* in *ey > p35* eye imaginal discs triggers ROS generation (D) and hemocyte recruitment (F). DHE and NimC were used as ROS indicator and hemocyte marker, respectively. Quantified in (N) and (O). Scale bars: 100 μm.

(G and H) *Duox* RNAi (H), but not *Nox* RNAi (G), can suppress *Toll-9*-induced overgrowth of *ey > p35* head capsules. Quantified in (M). The arrow in (G) highlights overgrown tissue with additional bristles.

(I–L) ROS generation and hemocyte clustering of *ey > p35,Toll-9* eye discs are suppressed by *Duox* RNAi (J–L) but not by *Nox* RNAi (I and K). DHE and NimC were used as ROS indicator and hemocyte marker, respectively. Quantified in (N) and (O).

(M) Quantification of the data in (A), (B), (G), and (H). Scoring criteria as in Figure 1E. At least 100 flies were scored for each genotype.

(N and O) Quantification of the DHE counts in (C), (D), (I), and (J) and hemocyte clusters in (E), (F), (K), (L). DHE counts and hemocyte clusters were counted across entire discs. Data were analyzed using one-way ANOVA with the Holm-Sidak test for multiple comparisons. Plotted is the mean ± SEM. **p < 0.01, **p < 0.001, and ****p < 0.0001. ns, not significant.

The genotypes of heads and eye discs are indicated above the panels. n = 4 (C), n = 4 (D), n = 7 (E), n = 12 (F), n = 6 (I), n = 6 (J), n = 7 (K), and n = 6 (L).

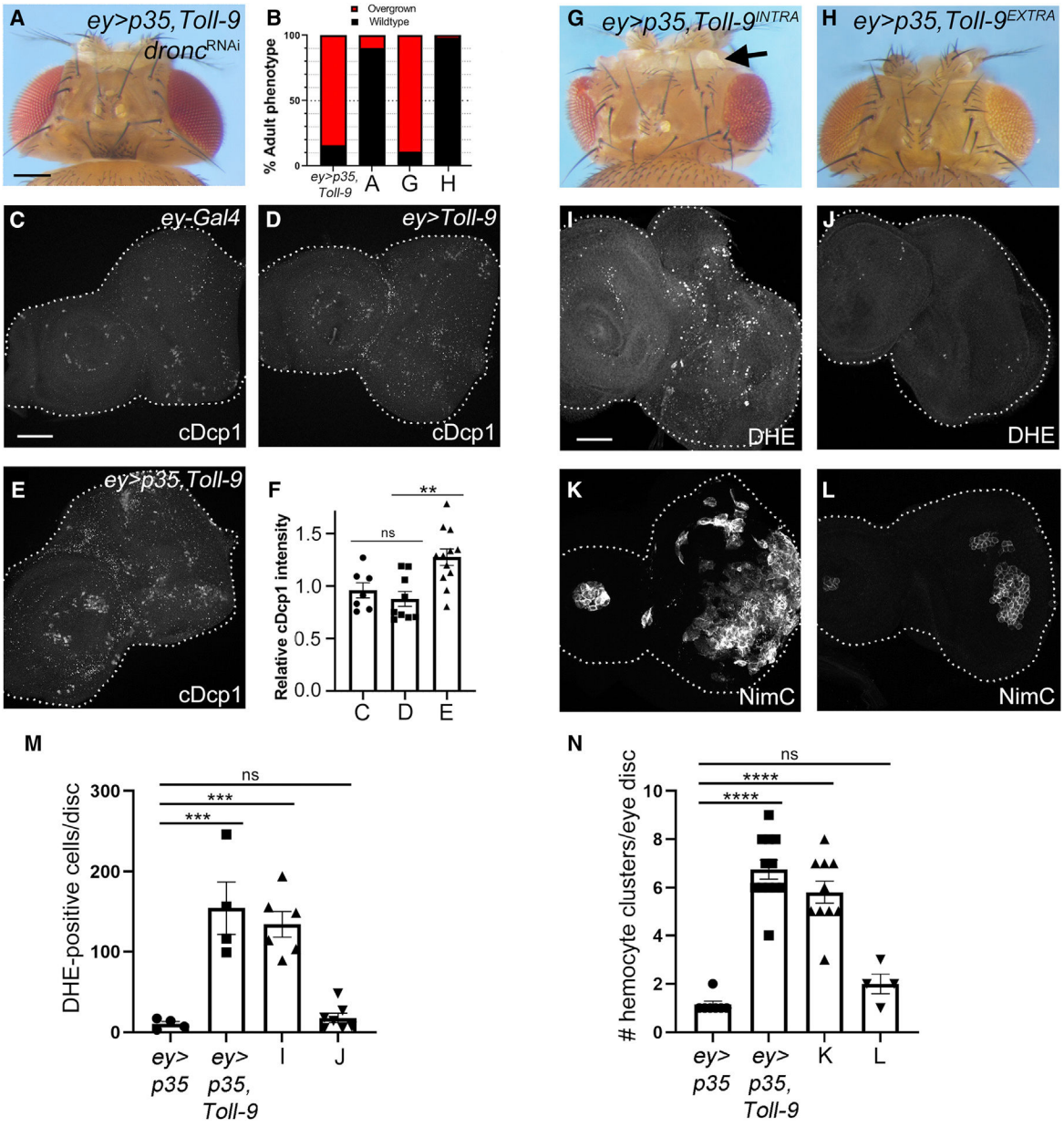

Figure 3. *dronc* is required and the intracellular domain of Toll-9 is sufficient for overgrowth of *ey > p35*-expressing head capsules

(A) RNAi knockdown of *dronc* suppressed *ey > p35,Toll-9*-induced overgrowth. Quantified in (B). Scale bar: 200 μm.

(B) Quantification of the data in (A), (G), and (H). Scoring criteria as in Figure 1E. At least 100 flies were scored for each genotype.

(C–E) cDcp1 labeling of imaginal eye discs of *ey-Gal4* (C), *ey > Toll-9* (D), and *ey > p35,Toll-9* (E) third-instar larvae. Quantified in (F). Scale bar: 100 μm.

(F) Quantification of the data in (C)–(E). cDcp1 labeling was measured across entire discs and normalized to disc size. Data were analyzed using one-way ANOVA with the Holm-Sidak test for multiple comparisons. Relative signal intensity is plotted ±SEM. **p < 0.01. ns, not significant. The following numbers of discs were analyzed: 7 (C), 9 (D), and 12 (E).

(G and H) Transgenic expression of the intracellular domain of *Toll-9* (*Toll-9^{INTRA}*) (G), but not the extracellular domain (*Toll9^{EXTRA}*) (H), causes overgrowth of the head capsule of *ey > p35*-expressing animals. Quantified in (M). The arrow in (G) highlights overgrown amorphic tissue. Scale bar: 200 μm.

(I–L) Transgenic expression of *Toll-9^{INTRA}*, but not *Toll-9^{EXTRA}*, triggers ROS generation (I and J) and hemocyte recruitment (K and L) in *ey > p35*-expressing eye imaginal discs. DHE and NimC were used as ROS indicator and hemocyte marker, respectively. Quantified in (M and N). Scale bar: 100 μm.

(M and N) Quantification of the data in (I) and (J) and in (K) and (L). DHE counts and hemocyte clusters were obtained across entire discs. Data were analyzed using one-way ANOVA with the Holm-Sidak test for multiple comparisons. Plotted is the mean ± SEM. ***$p < 0.001$ and ****$p < 0.0001$. ns, not significant.

The following numbers of discs were analyzed: 4 (*ey > p35* in M), 4 (*ey > Toll-9,p35* in M) 6 (I), 7 (J), 5 (*ey > p35* in N), 11 (*ey > Toll-9,p35* in N), 10 (K), and 4 (L).

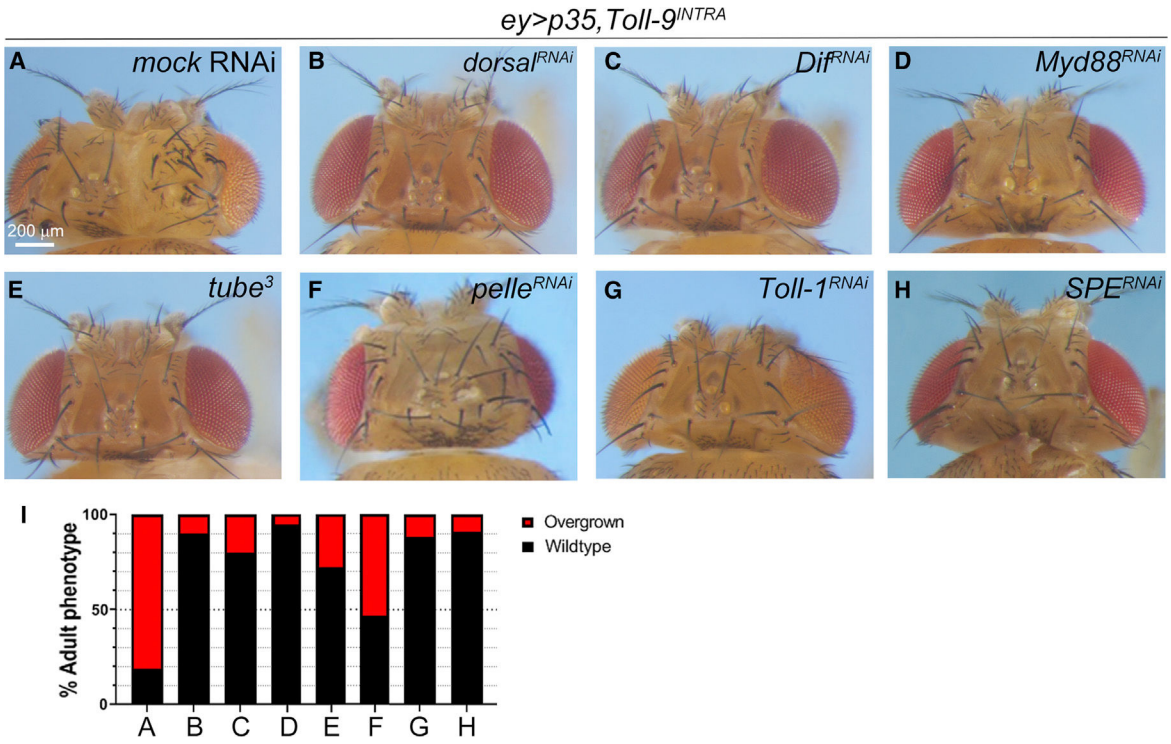

Figure 4. Canonical, intracellular Toll-1 signaling contributes to *ey > p35,Toll-9*-induced overgrowth

(A–C) *ey > p35,Toll-9*-induced overgrowth (A) is strongly suppressed by RNAi-mediated knockdown of *dorsal* (B) and *Dif* (C). Scale bar: 200 µm.

(D–H) RNAi-mediated knockdown of *Myd88* (D), *pelle* (F), *Toll-1* (G), and *SPE* (H) as well as a *tube* mutant (E) suppressed *ey > p35,Toll-9*-induced overgrowth.

(I) Quantification of the data in (A)–(H). Scoring criteria as in Figure 1E. At least 100 flies were scored for each genotype.

See also Figure S5.

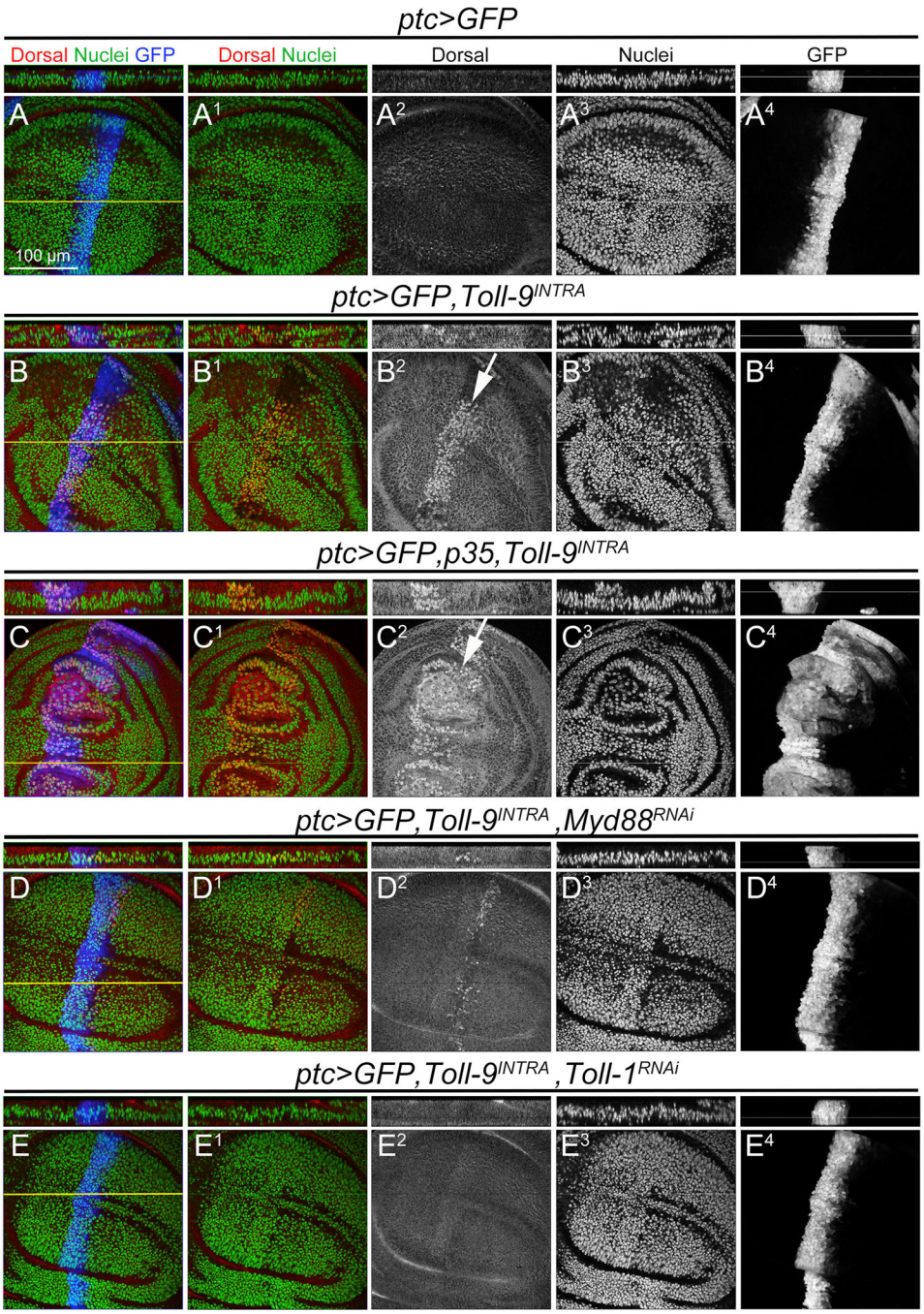

Figure 5. Toll-9-induced nuclear localization of Dorsal is dependent on canonical Toll-1 signaling

All wing imaginal discs were labeled with anti-Dorsal antibody (red). GFP is pseudo-colored in blue and highlights the *ptc* domain. Nuclei (green) were stained with Hoechst. Scale bar: 100 μm. The yellow lines in merged panels indicate the regions from which orthogonal sections (shown above panels) were derived. At least 20 wing imaginal discs were analyzed per genotype.

(A) A control (*ptc > GFP*) wing imaginal disc.

(B and C) Misexpression of *Toll-9* results in nuclear localization of Dorsal in *ptc > GFP,Toll-9^{INTRA}* (B) and *ptc > GFP,p35,Toll-9^{INTRA}* (C) wing imaginal discs. White arrows point to nuclear Dorsal in the *ptc* expression domain. Notably, the *ptc* expression domain was significantly expanded in *ptc > GFP,p35,Toll-9^{INTRA}* (C) wing imaginal discs, confirming that in the presence of *p35*, expression of *Toll-9* induces overgrowth.
(D and E) RNAi knockdown of *Myd88* (D) and *Toll-1* (E) blocked Toll-9-induced nuclear localization of Dorsal.
See also Figure S6.

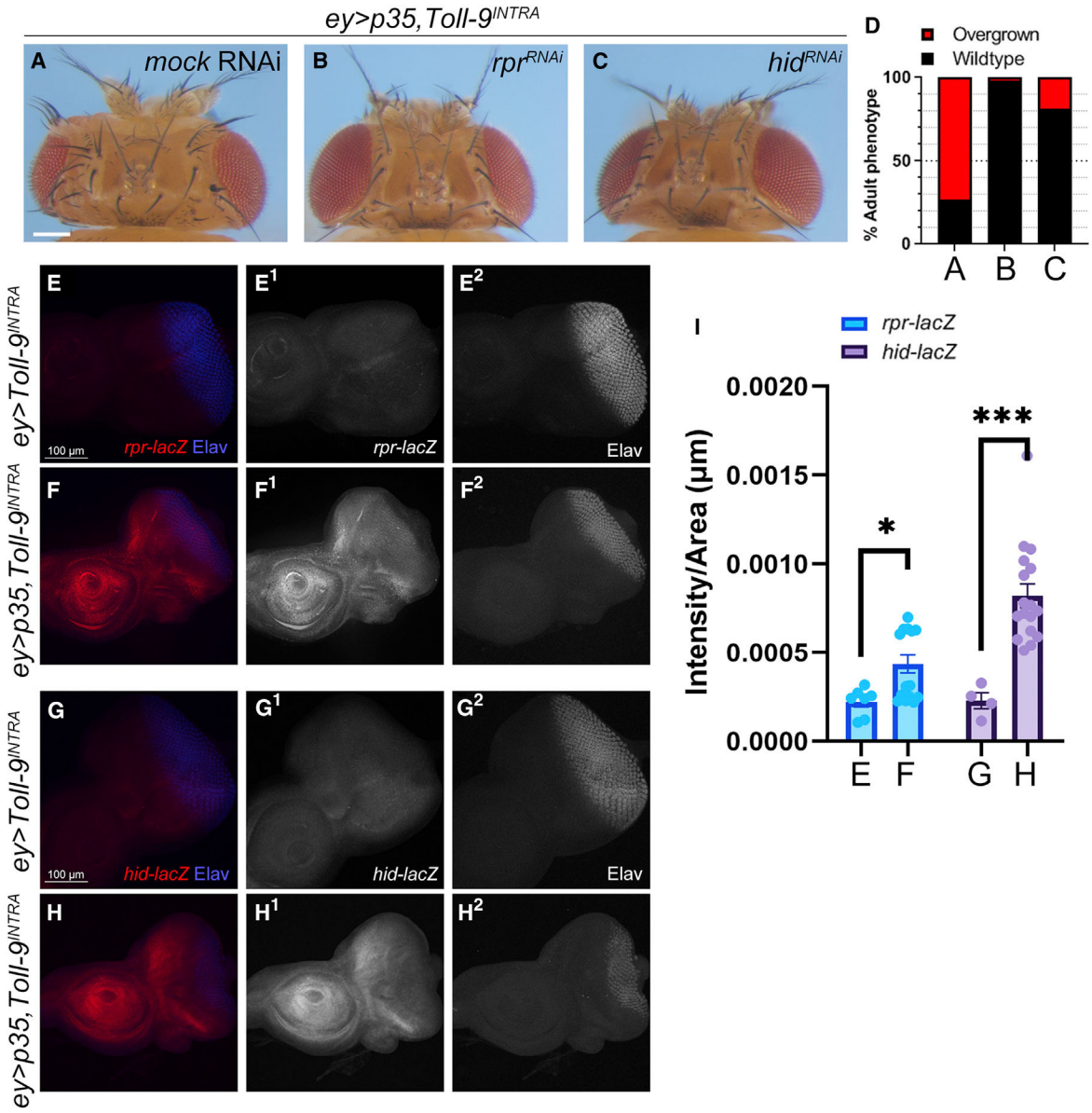

Figure 6. *Toll-9* induces expression of *reaper* and *hid* in *ey > p35* tissue

(A–C) *Toll-9*-induced overgrowth of *ey > p35* head capsules is suppressed by RNAi knockdown of *rpr* (B) and *hid* (C). Scale bar: 200 µm.

(D) Quantification of the data in (A)–(C). Scoring criteria as in Figure 1E. At least 100 flies per genotype were analyzed.

(E–H) *Toll-9*-induced expression of transcriptional reporters of *reaper* (*rpr-lacZ*) (E and F) and *hid* (*hid-lacZ*) (G and H) in *ey > p35* eye discs. Anti-beta-galactosidase was used to detect *lacZ* expression. Elav labels photoreceptor neurons. Scale bars: 100 µm.

(I) Quantification of the data in (E)–(H). An unpaired *t* test, two-tailed distribution, was performed to test the significance. Plotted is the mean intensity ± SEM. *p < 0.05 and ***p < 0.001.

The following numbers of discs were analyzed: 7 (E), 15 (F), 4 (G), and 17 (H). See also Figure S7.

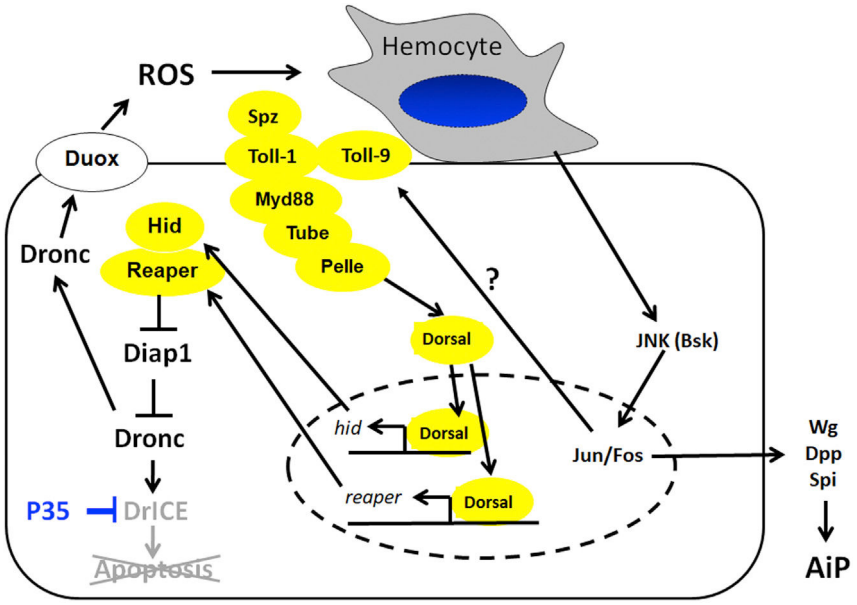

Figure 7. Model of Toll-9 function during undead AiP

Shown is an undead epithelial cell of a larval eye-antennal imaginal disc and an attached hemocyte. The interactions revealed in this paper are highlighted in yellow. Toll-9 engages a Toll-1-dependent intracellular pathway, culminating in the nuclear translocation of the NF-κB factor Dorsal, which directly or indirectly induces expression of *reaper* and *hid*. Previously shown interactions including the activation of Duox, recruitment of hemocytes, and activation of JNK (Amcheslavsky et al., 2018; Fogarty et al., 2016) are also shown. Wg, Dpp, and Spi are mitogens produced by undead cells for AiP.

KEY RESOURCES TABLE

REAGENT or RESOURCE	SOURCE	IDENTIFIER
Antibodies		
Mouse monoclonal anti-NimC antibody	Dr. Istvan Ando	RRID: AB_2568423
Dorsal	Developmental Studies Hybridoma Bank (DSHB)	DSHB Cat# anti-dorsal 7A4; RRID:AB_528204
Mmp1	DSHB	DSHB Cat# 3A6B4; RRID:AB_579780
Wingless	DSHB	DSHB Cat# 4d4; RRID:AB_528512
Elav	DSHB	DSHB Cat# Rat-Elav-7E8A10 anti-elav; RRID:AB_528218
Mouse monoclonal anti-β-Galactosidase	DSHB	DSHB Cat# 40–1a; RRID:AB_528100
Cleaved Dcp-1 (Asp176)	Cell Signaling Technology	Cat# 9578; RRID:AB_2721060
Chemicals, peptides, and recombinant proteins		
Dihydroethidium (DHE)	Invitrogen	Cat#D23107
H2DCF-DA	Molecular Probes	Cat#C6827
Vectorshield with DAPI	Vector Laboratories	Cat#H-1200; RRID: AB_2336790
Hoechst 33342	Invitrogene	Cat#H3570
Experimental models: Organisms/strains		
Drosophila melanogaster: Toll-9^{v17}	this study	N/A
Drosophila melanogaster: UAS-Toll-9	this study	N/A
Drosophila melanogaster: UAS-Toll-9^{INTRA}	this study	N/A
Drosophila melanogaster: UAS-Toll-9^{INTRA}	this study	N/A
Drosophila melanogaster: UAS-Toll-9 RNAi	Bloomington *Drosophila* Stock Center (BDSC)	BDSC 30535 FlyBase: FBst0030535
Drosophila melanogaster: UAS-Toll-9 RNAi	Vienna Drosophila Resource Center (VDRC)	VDRC v36308 FlyBase: FBst0461624
Drosophila melanogaster: UAS-Toll-9 RNAi	VDRC	VDRC v109635 FlyBase: FBst0481299
Drosophila melanogaster: UAS-Dif RNAi	VDRC	VDRC v100537 FlyBase: FBst0472410
Drosophila melanogaster: UAS-dorsal RNAi	VDRC	VDRC v105491 FlyBase: FBst0477317
Drosophila melanogaster: UAS-dorsal RNAi	BDSC	BDSC 34938 FlyBase: FBst0034938
Drosophila melanogaster: UAS-MyD88 RNAi	VDRC	VDRC v106198 FlyBase: FBst0478023
Drosophila melanogaster: UAS-pelle RNAi	VDRC	VDRC v103774 FlyBase: FBst0475632
Drosophila melanogaster: UAS-Toll-1 RNAi	VDRC	VDRC v100078 FlyBase: FBst0471952
Drosophila melanogaster: UAS-reaper RNAi	BDSC	BDSC 51846 FlyBase: FBst0051846
Drosophila melanogaster: UAS-hid RNAi	VDRC	VDRC v7912 FlyBase: FBst0470883
Drosophila melanogaster: UAS-dronc RNAi	VDRC	FlyBase: FBst0472297; VDRC v100424
Drosophila melanogaster: UAS-bsk RNAi	VDRC	VDRC v34138 FlyBase: FBst0460476
Drosophila melanogaster: UAS-Luciferase RNAi	BDSC	BDSC 31603 FlyBase: FBst0031603
Drosophila melanogaster: 4kb rpr-lacZ	Hermann Steller	FlyBase: FBal0105175
Drosophila melanogaster: hid[10–1kb]-lacZ	this study	N/A
Drosophila melanogaster: UAS-Toll-1	Tony Ip	FlyBase : FBal0181209

REAGENT or RESOURCE	SOURCE	IDENTIFIER
Drosophila melanogaster: UAS-SPE RNAi	VDRC	VDRC v104906 FlyBase: FBst0476734
Drosophila melanogaster: UAS-spz^{Act}	Laura Johnson	FlyBase: FBal0138129
Drosophila melanogaster: UAS-Duox RNAi (line #44)	Won-Jae Lee	FlyBase: FBal0190061
Drosophila melanogaster: UAS-Nox RNAi (line #4)	Won-Jae Lee	FlyBase: FBal0191562
Drosophila melanogaster: TRE-RFP	Dirk Bohmann	FlyBase: FBst0059011
Oligonucleotides		
Toll-9, Forward: 5′CCATTACAAGCACTATAGG	this study	N/A
Toll-9, Reverse: 5′-GACCTCTTCGGCCTCTTC	this study	N/A
RP-49: Forward: 5′-CCAGTCGGATCGATATGCTAA	this study	N/A
RP-49: Reverse: 5′-ACGTTGTGCACCAGGAACTT	this study	N/A
Software and algorithms		
Photoshop	Adobe	Version 2021
GraphPad Prism Software	GraphPad	Version 9
Zen imaging software	Carl Zeiss AG	Version 3.1